





Article

The Impacts of Micronutrient Fertility on the Mineral Uptake and Growth of *Brassica carinata*

Paul Cockson ^{1,*} , Patrick Veazie ¹ , Matthew Davis ¹, Gabby Barajas ¹, Angela Post ² , Carl R. Crozier ², Ramon G. Leon ² , Robert Patterson ² and Brian E. Whipker ¹

¹ Department of Horticultural Science, North Carolina State University, Raleigh, NC 27695, USA; pveazie@ncsu.edu (P.V.); mdavis14@ncsu.edu (M.D.); gbaraja@ncsu.edu (G.B.); bwhipker@ncsu.edu (B.E.W.)

² Department of Crop and Soil Sciences, North Carolina State University, Raleigh, NC 27695, USA; arricha3@ncsu.edu (A.P.); ccrozier@ncsu.edu (C.R.C.); rleon@ncsu.edu (R.G.L.); bob_patterson@ncsu.edu (R.P.)

* Correspondence: pcockso@ncsu.edu

Abstract: Many abiotic factors impact the yield and growth of *Brassica carinata* (commonly referred to as carinata or Ethiopian mustard). Very little is known about carinata and how mineral nutrients impact its growth, and more specifically, the sufficiency values for fertility over the plant's growth cycle and life stages. This study explored the impacts that plant nutrients, specifically micronutrients, can have on the growth and development of carinata over its distinct life stages (rosette, bolting, flowering, and pod set). Plants were grown under varying micronutrient concentrations (0, 25, 50, 75, 87.5, and 100%) of a modified Hoagland's solution. Data were collected on plant height, canopy diameter, leaf tissue mineral nutrient concentrations, and biomass. The results demonstrated that micronutrient fertility has profound impacts on the production of *Brassica carinata* during different life stages. Boron (B) exclusion had the greatest impact on the growth and reproduction of *Brassica carinata*, with the death of the apical meristem that resulted in a lack of siliques or seeds at the lowest rate. Optimal relative elemental leaf tissue concentrations varied among micronutrient fertility concentrations and life stages. Certain elements exhibited linear increases in nutrient leaf tissue accumulation as solution concentration increased without reaching a maximum concentration during specific life stages. Other life stages and/or elements produced distinct plateau leaf tissue mineral concentrations despite increasing fertility treatment concentrations such as B in the rosette stage (47.2–50.0 mg·kg⁻¹), copper (Cu) (bolting stage at 6.62–7.57 mg·kg⁻¹), zinc (Zn) (bolting stage at 27.47–39.87 and flowering at 33.98–43.50 mg·kg⁻¹), molybdenum (Mo) (flowering stage at 2.42–3.23 mg·kg⁻¹), and manganese (Mn) (bolting stage at 117.03–161.63 mg·kg⁻¹). This work demonstrates that *Brassica carinata* has different fertility demands and will accumulate differing leaf tissue concentrations during its life stages. This work serves as a baseline for further uptake and partitioning work for *Brassica carinata*.

Keywords: oilseed; Ethiopian mustard; fertility; life cycle; nutrients; rates; symptomology; foliar; aviation; biofuel; biodiesel



Citation: Cockson, P.; Veazie, P.; Davis, M.; Barajas, G.; Post, A.; Crozier, C.R.; Leon, R.G.; Patterson, R.; Whipker, B.E. The Impacts of Micronutrient Fertility on the Mineral Uptake and Growth of *Brassica carinata*. *Agriculture* **2021**, *11*, 221. <https://doi.org/10.3390/agriculture11030221>

Academic Editor: Emanuele Radicetti

Received: 19 January 2021

Accepted: 1 March 2021

Published: 8 March 2021

Publisher's Note: MDPI stays neutral with regard to jurisdictional claims in published maps and institutional affiliations.



Copyright: © 2021 by the authors. Licensee MDPI, Basel, Switzerland. This article is an open access article distributed under the terms and conditions of the Creative Commons Attribution (CC BY) license (<https://creativecommons.org/licenses/by/4.0/>).

1. Introduction

Over the past few decades, concerns of global climate change have resulted in increased attention and policy directed toward reducing or mitigating CO₂ emissions. One such mitigation policy is the diversification of the sources of fuel, creating a more robust and secure energy portfolio. For transportation, liquid biofuels are attractive due to their simple incorporation into existing motors and distribution infrastructure.

A specific priority is the development of renewable sources of aviation fuel. Aviation emissions are problematic given they produce CO₂ at high altitudes where CO₂ has a

longer persistence (Govardhan et al.) [1–4]. Plant lipid-sourced biofuels already have an established precedent in the form of soybean- and corn-derived ethanol and biodiesels [5–7]. Another important oil crop exists in the Brassicaceae family of oilseed crops. These Brassica and biologically derived biofuels played an important part in the energy system during increases in petroleum prices. Concerns about food or feed crops and degradation of sensitive landscapes are leading to policies favoring second-generation biofuels, which would consider global carbon (C) sequestration as well as other environmental and socioeconomic issues [8]. A research group in the southeastern U.S. is evaluating the oilseed crop *Brassica carinata*, also known as Ethiopian mustard [9]. This crop could be grown at a time when many farms are in a winter fallow state, thus minimizing food/feed crop displacement. It also has a unique oil profile [10] that has a higher concentration of mid-chain (MCFA), long-chain (LCFA), and very-long-chain fatty acids (VLCFA) than other oilseed Brassicas. These fatty acids, after refinement, produce a fuel molecule readily substitutable for petroleum-derived aviation fuel [1,2,5,7].

Despite the success already observed in aviation biofuels produced from *carinata*, some challenges remain for the acceptance of this as a commercial crop. For example, abiotic stresses can have deleterious impacts on yield, plant growth, and oil quantity and quality, which may disrupt the continuous supply chain of a bio-derived fuel and other co-products. One such abiotic stress is that of plant nutrients and fertility. Plants require certain macro and micronutrients to optimize growth, yield, and to complete their lifecycle [11]. These nutrients have a direct impact on yield, especially in Brassicas [12,13]. Additionally, Brassicas have distinct life stages, each requiring different nutrients to ensure adequate development and yield.

Brassicas undergo distinct phases of their growth habit after germination (*carinata* growth stages supplementary data) [6,14,15]. During different life stages, fertility requirements will vary largely due to changes in growth rate and developing sources and sinks. These differences were explored to elucidate the differences in plant nutrient requirements at different life stages.

In addition to different fertility needs based on life stage, different essential nutrient demands exist in Brassicas. For example, during the bolting phase, rapid cell polarization and expansion necessitate a higher use of elements that aid the expansion and stabilization of the cell wall. Boron is primarily found in the cell wall contained within the B-dimeric rhamnogalacturonan II (RG-II) complex [16]. Within this complex, both boron (B) and calcium (Ca) help to stabilize the structure and allow the complex to carry out its function of creating Ca ion bridges between the pectin chains within the cell wall [16,17] when the RG-II complex was monomeric and the cell walls swelled rather than differentiating polarly [16]. Given the stabilizing nature of the role the RG-II complex plays within the cell wall and stabilizing the pectin matrix, under Ca- or B-deficient conditions, cells cannot expand properly or directionally. The bolting phase produces the flower spikelet and undergoes rapid cell development; thus, any limitation of B or Ca can directly impact flower formation and, by extension, siliques and seeds.

The impact of B on yield as a foliar application resulted in a 10% increase in yield when applied at the early flowering stage of canola, a similar oilseed Brassica [18]. Another study in 2009 [19] looked at the impacts of micronutrients (B, molybdenum (Mo), and zinc (Zn)) on seed yield in *Brassica napus* L. When B was applied, there was a 46% increase in seed yield even when compared to the Mo and Zn treatments. This suggests that B is a limiting factor in seed formation and yield. When all three micronutrients were applied together, the greatest yield was observed at 68% above the control. There was a significant yet small increase in oil concentration and oil quality in all treatments.

Iron (Fe) is important to plant growth and development and is integral to many enzymatic functions. One of the most important functions of Fe is in the redox system through the biosynthesis of heme coenzymes, the chlorophyll molecule, and iron-sulfur proteins [11,20]. Another important function of Fe is in the development of chloroplasts. Within the chloroplasts, under Fe-deficient conditions, protein synthesis is greatly re-

duced [21]. Additionally, the thylakoid membrane contains around 20 Fe constituents that are involved in photosystem I and II (PS I and II) [22,23]. In addition to the deleterious impact Fe deficiency can have on the production of photosynthates, which have a direct impact on lipid metabolism, Fe deficiency can cause lipid peroxidation in some Brassicas [24]. This would have a direct impact on the stability and polymerization of lipid molecules as well as seed viability and storage.

Copper (Cu) is also an essential plant micronutrient. Copper is primarily used within plants in the photosystem II pathway as a structural part of the enzyme plastocyanin [25]. Additionally, Cu is involved in the lignification process of the cell walls, though the exact mechanism remains unclear [25].

Zinc also plays an important role in plants. It is present in many plant enzymes, plays a role in mitigating the production of ethanol under aerobic conditions within meristematic regions, is involved in the carbonic anhydrase pathway, and is integral in carbohydrate metabolism as an activator of fructose 1,6-bisphosphatase and aldolase [26–29]. Additionally, Zn is related to the stability, integrity, and longevity of membranes. In particular, Zn helps to bind with different complexes in order to create polypeptide and cysteine structures, which in turn help to guard against harmful oxidative processes with regard to lipids [30,31].

Molybdenum is an element that is primarily important to nodulating crops such as legumes, which form symbiotic associations with atmospheric nitrogen (N₂)-fixing bacterium. Additional roles of Mo are to aid in the assimilation and use of N [32]. A symptom known as whiptailing has been observed in Brassicas under Mo-deficient conditions in which the reproductive leaves appear elongated and distorted [33].

Manganese has a wide impact on plant growth and development, given its role within photosystem II and the superoxide dismutase molecule (MnSOD). Within PS II, under Mn-deficient conditions, the true level of chlorophyll will only result in a slight decrease. When Mn is deficient, the O₂ evolution within younger developing leaves can decrease by almost half [34–36]. The impacts of Mn shortages on the metabolic activities of the plant can be severe. Within plants, the thylakoid membrane can be deleteriously impacted due to a shortage of or degradation of glycolipids and polyunsaturated fatty acids [37]. The impacts of Mn can be observed within seeds and developing embryos [38]. Seed proteins and lipids are impacted inversely as Mn concentrations increase, with seed oil being higher under increasing Mn concentrations within the plant [35]. Additionally, the types of fatty acids within the seeds can be impacted under different Mn concentrations. Within seeds, oleic acid concentration is typically higher under greater Mn conditions, with linoleic acid following an inverse relationship to oleic acid [35].

While micronutrients are required in smaller quantities within the plant than macronutrients, they are still necessary elements [39]. When levels of a microelement fall below a critical range, negative impacts are observed on plant growth and development, physiological functions and pathways, metabolites, and seed and embryo development [40]. To rectify or avoid these negative impacts, proper fertility must be administered to plants during all stages of development. This work seeks to explore the impacts of micronutrients on the growth and development of a new and emerging biofuel oilseed crop *B. carinata*. The optimal micronutrient fertility ranges were explored by supplying each micronutrient at reducing fertility levels based on a modified Hoagland's solution. The impacts on total plant aboveground biomass as well as leaf tissue concentration were cataloged. At each of the distinct life stages of the crop (rosette stage, bolting, and flowering), the above metrics were taken.

2. Materials and Methods

2.1. Seed Sow

Brassica carinata Avanza 641 (Agrisoma, Gatineau, QC, Canada) seeds were sown on 3 November 2018 into 72-cell plug trays filled with a substrate mix of 80:20 (v:v) Canadian sphagnum peat moss (Conrad Fafard, Agawam, MA, USA) and horticultural grade perlite

(Perlite Vermiculite Packaging Industries, Inc., North Bloomfield, OH, USA). The substrate mix was amended with dolomitic lime at 8.875 kg/m^3 (Rockydale Agricultural, Roanoke, VA, USA) and wetting agent (Aquatrols, Cherry Hill, NJ, USA) at 600 g/m^3 . The premade substrate mix ensured no micronutrient charge or contaminants were present in the seeding substrate. Seedlings were then grown at $22.8 \pm 2.8 \text{ }^\circ\text{C}$ day/night (D/N) temperatures ($73.0 \pm 5.0 \text{ }^\circ\text{F}$) in a glass greenhouse in Raleigh, NC, USA (35.8° N Latitude) under a mist bench set at irrigation intervals (5 s every 3 min). After the second true leaf emerged, the plants were removed from mist and hand irrigated with a nurse nutrient solution (33.4 g KNO_3 , 33.4 g $\text{Ca}(\text{NO}_3)_2 \cdot \text{H}_2\text{O}$, 6.6 g KH_2PO_4 , 13.2 g $\text{MgSO}_4 \cdot 7\text{H}_2\text{O}$ in 20 L H_2O per 100 L deionized (DI) H_2O).

Plugs were then grown out and hardened until they developed four true leaves, after which time, they were transplanted on 13 December 2018 into 15.24 cm diameter (1.76 L) plastic pots filled with acid-washed silica-sand (Millersville #2 (0.8 to 1.2 mm diameter) from Southern Products and Silica Co., Hoffman, NC, USA) [39]. Each pot received one rooted plug. At transplant fertility, treatment regimens started.

2.2. Transplant and Micronutrient Fertility Treatments

After transplant, the plants were grown at $15.5/12.8 \pm 2.8 \text{ }^\circ\text{C}$ D/N temperatures ($59.9/55.0 \pm 5.0 \text{ }^\circ\text{F}$). On 7 February 2019, temperatures were increased to $18.3/15.5 \pm 3.1 \text{ }^\circ\text{C}$ D/N ($65/60 \pm 5.6 \text{ }^\circ\text{F}$) to encourage bolting, with the bolting harvest occurring on 15 February 2019 and the flowering harvest occurring 1 March 2019. Plants were grown in an automated, recirculating irrigation system constructed from 10.2 cm diameter polyvinyl chloride (PVC) pipe (Charlotte Plastics, Charlotte, NC, USA), fit with 12.7 cm diameter openings to hold the pots (Henry et al.) [39]. Plants were distributed into rows capable of holding either 8 or 6 pots with 6 rows blocked per group and 4 groups per bench with a total of four benches in the greenhouse. Each row received a different micronutrient fertility treatment with treatments distributed among benches, blocks, and lines using a randomized block design. Fertility micronutrient treatments were sub-divided into different concentrations (0, 25, 50, 75, 87.5, and 100%) of a modified Hoagland's solution [39,41,42]. Control plants ($n = 4$ per each data collection) were grown with (macronutrient concentrations in mM) 15 nitrate-nitrogen (NO_3^-), 1.0 phosphate-phosphorus (H_2PO_4^-), 6.0 potassium (K^+), 5.0 calcium (Ca^{2+}), 2.0 magnesium (Mg^{2+}), and 2.0 sulfate-sulfur (SO_4^{2-}) plus (micronutrient concentrations in μM) 72 Fe (Fe^{2+}), 18 Mn (Mn^{2+}), 3 Cu (Cu^{2+}), 3 Zn (Zn^{2+}), 45 B (BO_3^{3-}), and 0.1 Mo (MoO_4^{2-}) [41]. Micronutrients were altered based on the above baselines set as 100%, with each consecutive micronutrient being lessened by the above percentages. A complete listing of nutrients and rates is presented in Table 1. All nutrient solutions were tested to confirm elemental concentrations using the North Carolina Department of Agriculture and Consumer Services (NCDA) testing lab using 50 mL of the solutions (NO_3 analyzed using spectrophotometry, all other elements determined using inductively coupled plasma mass spectrometry (ICP). More details can be found here) after letting the concentrations sit for 48 h after mixing (Raleigh, NC, USA). Upon mixing more fertilizer solutions, each new batch was visually inspected for precipitates, and the pH and electrical conductivity (EC) were tested to ensure the values were within the desired ranges.

Plants were drip irrigated using their assigned modified micronutrient solutions using a sump-pump (model 1A, Little Giant Pump Co., Oklahoma City, OK, USA) system. Irrigations occurred every hour and ran for one minute between 6:00 and 19:00 h. Irrigation solution drained from the pot and was captured for reuse, with solutions being emptied and replenished weekly [39]. For more details on the modified Hoagland's solution and the setup, please refer to Barnes et al. [42].

Table 1. Concentrations for modified Hoagland’s solution used to explore the impacts of varying micronutrients on the growth of *Brassica carinata* over its life stages.

	Micronutrient Fertility Rate (%) ¹											
	0.0		25.0		50.0		75.0		87.5		100.0	
	$\mu\text{mol}\cdot\text{L}^{-1}$	ppm	$\mu\text{mol}\cdot\text{L}^{-1}$	ppm	$\mu\text{mol}\cdot\text{L}^{-1}$	ppm	$\mu\text{mol}\cdot\text{L}^{-1}$	ppm	$\mu\text{mol}\cdot\text{L}^{-1}$	ppm	$\mu\text{mol}\cdot\text{L}^{-1}$	ppm
Iron (Fe) ²	0.00	0.00	18.00	1.01	36.00	2.01	54.00	3.02	63.00	3.52	72.00	4.02
Manganese (Mn) ²	0.00	0.00	4.50	0.25	9.00	0.50	13.50	0.74	15.75	0.87	18.00	0.99
Zinc (Zn) ²	0.00	0.00	0.75	0.05	1.50	0.10	2.25	0.15	2.63	0.18	3.00	0.20
Copper (Cu) ²	0.00	0.00	0.75	0.05	1.50	0.10	2.25	0.14	2.63	0.17	3.00	0.19
Boron (B) ²	0.00	0.00	11.25	0.12	22.50	0.25	33.75	0.37	39.38	0.43	45.00	0.49
Molybdenum (Mo) ²	0.00	0.00	0.025	0.0025	0.050	0.005	0.075	0.0075	0.088	0.0088	0.100	0.01

¹ Values indicate the adjusted fertility rate provided from a modified Hoagland’s solution with all elements held constant except the adjusted microelement being studied. These values are expressed as a percentage of the standard Hoagland’s solution [41]. ² Values given for each element listed in $\mu\text{mol}\cdot\text{L}^{-1}$. To convert $\mu\text{mol}\cdot\text{L}^{-1}$ to parts per million (ppm), multiply by the molecular weight and divide by 1000.

Plants were grown in their respective micronutrient treatments until either visual nutrient deficiency symptoms were observed or the respective physiological stage was observed in over 50% of the control plants (100% modified Hoagland’s solution). Physiological stages for harvest were set at the rosette, bolting, flowering, and pod-set stages. Stages were determined using the decimal code (1.5–1.9: rosette, 3.0–3.3: bolting, 6.5: full flowering, 8.9–9.5: pod set) developed by the Southeast Partnership for Advanced Renewables from *Carinata* (SPARC see citation) working group (Figure S1).

2.3. Plant Harvest and Data Collection

After the onset of initial visual deficient symptoms of each micronutrient treatment occurred, four symptomatic plants were selected and sampled. If visual symptoms did not develop, plants were harvested when over 50% of control plants reached physiological and morphological changes based on life cycle (Figure S1). After sampling of the four replicates, the remaining plants ($n = 12$) were grown to document symptomological and nutrient stresses into the remaining physiological stages. Thus, four more replicates were harvested when 50% of the control plants reached the bolting stage (Figure S1), likewise for the full-flowering and pod-set stages.

For the four harvested replicates, most recently matured leaves were sampled to evaluate the critical micronutrient tissue concentrations for each fertility treatment and concentration. Plants were destructively harvested, and the most recently matured leaves were initially rinsed with deionized water, then washed in a solution of 0.5 M hydrochloric acid (HCl) for 1 min and again rinsed with deionized (DI) water [39]. The remaining shoot tissue was harvested separately, and roots were discarded.

Each harvest followed the above protocol with the exception of the final harvest (8.9–9.5: pod set; Figure S1), which had total dry mass taken and pods removed. For this harvest, the total dry weight was calculated by adding the plant biomass and the pod dry weights together. The remaining harvests had plant biomass data, symptomology, and most recently matured leaf tissue analysis taken for data at their respective physiological and morphological stages.

Upon sampling, the plant tissues were dried at 70 °C for 96 h, and the dry mass was weighed and recorded. After drying, leaf tissue was ground in a Foss Tecator Cyclotec™ 1093 sample mill (Analytical Instruments, LLC; Golden Valley, MN, USA; ≤ 0.5 mm sieve). The ground tissue was then placed in vials containing ~8 g of tissue and sent for analysis to AgSource Laboratories (Lincoln, NE, USA). A composite sample was taken from the vial ($0.250 \text{ g} \pm 0.003 \text{ g}$) and digested with nitric acid (12 M) at 60 °C. After the nitric acid digestion, 3 mL of 30% hydrogen peroxide was added to the sample, and further digestion occurred at 120 °C. Upon cooling, the sample was then diluted to 25 mL using a 20% hydrochloric acid solution. Analysis occurred using an ICP-OES machine (Agilent 5110; Santa Clara, CA, USA) using a 0.5 mL loop.

Once tissue values and plant dry weights were obtained, data were analyzed using the SAS program (version 9.4; SAS Inst., Cary, NC, USA). All leaf tissue mineral nutrition

values and plant dry weights (tissue + rest of aboveground plant biomass) were subjected to GLM using PROC GLM. The GLM procedure calculated the differences in means of the total plant dry weight and element and used the concentration as the predictor. Means were subjected to Tukey's multiple comparison test. The resultant report indicated which samples were statistically different from each other and are reported in the summary Tables 1–6.

2.4. Data Analysis

Data were then subjected to first- and second-order polynomial regression using PROC REG. Regression models treated the leaf tissue concentration of the element as the y variable and the concentration of the modified Hoagland's solution fertility as the x variable. Each element was analyzed separately from the rest to eliminate any competition or enhancement that may have resulted from nutrient antagonisms or synergisms of uptake [43,44]. Regression models were compared, and the polynomial model, which resulted in the greatest statistical significance ($\alpha = 0.05, 0.01, 0.001$) and the greatest adjusted r^2 values were selected.

Tables were populated with the means from the statistical outputs above. Data are organized by element with concentrations modeling impacts on both dry weights and leaf tissue element concentrations. The data report the means of each dataset with the associated r^2 and adjusted r^2 , and regression polynomial equations can be found in the supplementary data (Tables S1–S6).

3. Results and Discussion

3.1. Boron (B)

Results varied by life stages and across B concentrations. The impacts of B deficiency were observed acutely at the $0.00 \mu\text{mol}\cdot\text{L}^{-1}$ B level. The plants grown under $0.0 \mu\text{mol}\cdot\text{L}^{-1}$ B did not reproduce due to the death of the apical meristem. Visual deficiency symptoms occurred at both the 0.0 and $11.25 \mu\text{mol}\cdot\text{L}^{-1}$ B concentrations across all life stages.

3.1.1. B Deficiency Symptomology

The first symptoms of B scarcity in *carinata* manifested as general stunting and distortion of newly expanding leaves (Figure S2). The upper foliage of the plant folded inward and downward, creating a wilted leaf appearance, whereas new growth was distorted, creating a wrinkled leaf effect. Petioles and midribs of upper foliage, as well as new growth, also developed cracking (Figures S3 and S4).

Under advanced B-deficiency conditions, the leaf margins cupped inward (Figure S4). As symptoms progressed, B deficiency resulted in the death of the growing tip (Figure S5) and the release of axillary shoots (Figure S6). As B continued to be limited, axillary shoots became necrotic, and the plant eventually died.

3.1.2. Rosette-Stage B Rates

Rosette plants varied in the distribution of their dry weights based on B fertility concentrations. Total plant dry weight increased as B concentrations increased (Table S1 and Table 2). The quadratic model accounted for 73.3% of the data when treating dry weight as the dependent variable and B fertility concentration as the predictor (Table S1). The lowest concentration ($0.00 \mu\text{mol}\cdot\text{L}^{-1}$ B) produced less biomass when compared to the next three highest concentrations ($11.25, 22.50, 33.75 \mu\text{mol}\cdot\text{L}^{-1}$) (Table S1). The two highest concentrations (39.38 and $45.00 \mu\text{mol}\cdot\text{L}^{-1}$ B) produced the greatest biomass when compared to all other values (Table 2).

Table 2. *Brassica carinata* plant dry weights (g) and leaf tissue concentration ($\text{mg}\cdot\text{kg}^{-1}$) based on boron (B) fertility treatments.

B Fertility ($\mu\text{mol}\cdot\text{L}^{-1}$) ^{1,2}	0.0	11.25	22.50	33.75	39.38	45.0
Plant Dry Weight (g)						
Rosette	1.35 A ***	5.44 B ***	5.20 B ***	5.55 B ***	9.33 C ***	8.53 C ***
Bolting	11.26 A **	26.28 AB **	38.21 B **	30.10 B **	35.56 B **	31.51 B **
Flowering	3.73 A ***	32.96 B ***	39.10 B ***	36.08 B ***	36.73 B ***	40.68 B ***
B Leaf Tissue Nutrient Concentrations ($\text{mg}\cdot\text{kg}^{-1}$)						
Rosette	9.39 A ***	47.20 B ***	48.46 B ***	49.40 B ***	49.45 B ***	50.00 B ***
Bolting	3.63 A ***	41.84 B ***	59.82 C ***	65.50 C ***	92.52 D ***	91.20 D ***
Flowering	11.41 A ***	70.10 B ***	79.20 BC ***	86.70 BC ***	111.64 D ***	98.52 CD ***
Comparison Boron Leaf Tissue Values ($\text{mg}\cdot\text{kg}^{-1}$)³						
	<i>Brassica carinata</i> ³			<i>Brassica napus</i> ⁴		
Rosette ³	13.4–26.2					
Bolting ³	10.0–18.8			15.0–54.0		
Flowering ³	6.5–19.1					

¹ Values indicate the adjusted fertility rate provided from a modified Hoagland's solution with all elements held constant except the adjusted microelement being studied [41]. ² *, **, or *** indicate statistically significant differences between sample means across a row based on *F*-test (proc GLM) at $p \leq 0.05$, $p \leq 0.01$, or $p \leq 0.001$, respectively. NS (not significant) indicates the *F*-test difference between sample means was $p > 0.05$. Values with the same letter indicate a lack of statistical significance, whereas values with different letters indicate statistically significant results. ³ Reference values from Seepaul et al. [6,14]. Values given are based on *Brassica carinata* leaf tissue samples from two growing seasons with samples taken based on plant life stages. ⁴ Reference values based on 50 mature leaves without petioles taken throughout the season from rosette stage to pod set. Values taken from *Brassica napus* leaf tissue values from Bryson et al. [45].

Leaf tissue B concentration exhibited a plateau at 11.25 $\mu\text{mol}\cdot\text{L}^{-1}$ B concentration. The lowest B concentration (0.00 $\mu\text{mol}\cdot\text{L}^{-1}$) contained 81.2% less B than the control at 45.0 $\mu\text{mol}\cdot\text{L}^{-1}$ B (Table 2). When modeling the impacts of B fertility on leaf tissue accumulation, a quadratic model provided the best interpretation of the variance within the study (Table S1).

Limited literature quantifies nutrient and dry weight concentrations of *Brassica sp.* at different growth stages, with two studies reporting a strong increase in final yield with B applications [46,47]. The lack of response in plant leaf tissue accumulation of B above the 11.25 $\mu\text{mol}\cdot\text{L}^{-1}$ concentration was most likely due to the use of B within the plant. Boron is used at a much higher concentration during periods of rapid cell expansion and growth. Boron is primarily found in the cell wall contained within the B-dimeric rhamnogalacturonan II (RG-II) complex [46]. Within this complex, both B and Ca help to stabilize the structure and allow the complex to carry out its function of creating calcium ion bridges between the pectin chains within the cell wall [46,48]. The RG-II complex was monomeric, and the cell walls swelled rather than differentiating polarly [46]. It may be that given the stabilizing nature of the role the rhamnogalacturonan II (RG-II) complex plays within the cell wall and stabilizing the pectin matrix, the cells may expand properly or directionally. This role may explain the early plateau observed in the leaf tissue B concentrations of the rosette stage.

3.1.3. Bolting-Stage B Rates

Bolting plants within the B treatments manifested visual deficiency symptoms only at the 0.00 $\mu\text{mol}\cdot\text{L}^{-1}$ concentration. Plants grown with 0.00 $\mu\text{mol}\cdot\text{L}^{-1}$ B resulted in young and expanding leaves with necrosis of the apical meristem (Figures S5 and S6). The

necrosis resulted in the proliferation of axillary shoots, which displayed stunting and severe distortion (Figures S2 and S4).

An increasing trend in total plant dry weights occurred from the 0.00 to 11.25 and 22.5 $\mu\text{mol}\cdot\text{L}^{-1}$ B rates. All concentrations greater than the 11.25 $\mu\text{mol}\cdot\text{L}^{-1}$ B were statistically similar, and all were greater as compared to 0.00 $\mu\text{mol}\cdot\text{L}^{-1}$ B treatment (Table 2). Regression analysis demonstrated a quadratic model provided greater explanatory power of the dependent variable when compared to a linear model (Table S1).

Leaf tissue B concentration exhibited a quadratic increase as B fertility increased (Table 2). With the two lowest concentrations (0.0 and 11.25 $\mu\text{mol}\cdot\text{L}^{-1}$ B) being statistically different from each other, the 22.50 and 33.75 $\mu\text{mol}\cdot\text{L}^{-1}$ B treatments were statistically similar, and the next two highest concentrations (39.38 and 45.00 $\mu\text{mol}\cdot\text{L}^{-1}$ B) as a pair also being statistically similar (Table 2). The highest B leaf tissue concentration occurred at the 39.38 $\mu\text{mol}\cdot\text{L}^{-1}$ B (Table 2). Whereas the linear and quadratic models were similar, the quadratic model should be used given a plateau in leaf tissue B was observed in both the rosette and flowering stages (Table S1).

These results indicate that during times of rapid cell growth and expansion, B requirements are much higher given B's role in cell development. The greater need for B resources was reported at the lowest B fertility concentration of 0.0, though plants did not exhibit a complete loss of yield, despite a small amount of B being applied to prevent complete yield loss [49]. Yang's work demonstrates that under-applying B can negatively impact plant biomass production and potentially result in complete yield loss if corrective measures are not taken.

3.1.4. Flowering-Stage B Rates

Flowering plants mirrored the bolting stage plateau at 11.25 $\mu\text{mol}\cdot\text{L}^{-1}$ B for dry weights (Table 2), indicating bolting and flowering carinata plants require the same concentrations of B fertility to maximize biomass production. Leaf tissue B concentration modeled an increasing trend as B concentrations increased (Table 2). Leaf tissue B concentrations differed significantly between the lowest concentration and the remaining concentrations. A quadratic model accounted for 84% of the variation within the dataset when treating leaf tissue B as the dependent variable and B fertility concentration as the predictor (Table S1).

As stated earlier, B is important for proper cell wall formation and cellular development and expansion. Thus, the lack of silique and seed formation at the lowest rate (0.00 $\mu\text{mol}\cdot\text{L}^{-1}$ B) indicates concentrations between 11.25 and 22.50 $\mu\text{mol}\cdot\text{L}^{-1}$ B optimized biomass production; however, in soil conditions, the recommendations will be refined further.

3.2. Iron (Fe)

Iron treatment values displayed inconsistent results despite visual symptomology being present at the lowest (0.0 $\mu\text{mol}\cdot\text{L}^{-1}$ Fe) fertility concentration at all life stages.

3.2.1. Fe Deficiency Symptomology

The first symptom of Fe scarcity in carinata was interveinal chlorosis of the upper foliage (Figure S7). During the bolting stage, upper leaves along the flower spikelet displayed interveinal chlorosis, which continued into flowering and pod set (Figure S8). Under Fe-deficient conditions, nutrient stress was present at all carinata life stages.

3.2.2. Rosette-Stage Fe Rates

Rosette plants varied in the distribution of their dry weights based on Fe fertility concentrations. Total plant dry weight increased as Fe concentrations increased (Table S2 and Table 3). Plants grown at the lowest concentration (0.0 $\mu\text{mol}\cdot\text{L}^{-1}$) were significantly smaller than at all other concentrations. The quadratic model interpreted the greatest amount (0.67) of the variance in plant dry weights (Table S2).

Table 3. *Brassica carinata* plant dry weights (g) and leaf tissue concentration (mg·kg⁻¹) based on iron (Fe) fertility treatments.

Fe Fertility (μmol·L ⁻¹) ¹	0.0	18.0	36.0	54.0	63.0	72.0
Plant Dry Weight (g)						
Rosette ²	0.97 A ***	5.80 B ***	7.58 BC ***	5.62 B ***	8.92 C ***	8.53 C ***
Bolting ²	26.91 AB **	33.85 A **	13.00 B **	23.91 AB **	30.48 A **	31.51 A **
Flowering ²	31.47 A NS	41.06 A NS	27.16 A NS	40.30 A NS	36.82 A NS	40.68 A NS
Fe Leaf Tissue Nutrient Concentrations (mg·kg⁻¹)						
Rosette ²	73.73 C ***	60.64 A ***	64.77 AB ***	69.35 BC ***	65.03 AB ***	74.83 C ***
Bolting ²	46.07 A ***	49.19 A ***	49.98 A ***	59.18 A ***	113.77 B ***	66.00 A ***
Flowering ²	43.67 A **	57.97 A **	53.57 A **	70.72 AB **	83.53 B **	56.40 A **
Comparison Fe Leaf Tissue Values (mg·kg⁻¹)³						
	<i>Brassica carinata</i> ³			<i>Brassica napus</i> ⁴		
Rosette ³	67.6–595.3					
Bolting ³	51.9–226.0			30.0–200.0		
Flowering ³	38.4–172.2					

¹ Values indicate the adjusted fertility rate provided from a modified Hoagland's solution with all elements held constant except the adjusted microelement being studied [41]. ² *, **, or *** indicate statistically significant differences between sample means across a row based on *F*-test (proc GLM) at $p \leq 0.05$, $p \leq 0.01$, or $p \leq 0.001$, respectively. NS (not significant) indicates the *F*-test difference between sample means was $p > 0.05$. Values with the same letter indicate a lack of statistical significance, whereas values with different letters indicate statistically significant results. ³ Reference values from Seepaul et al. [6,14]. Values given are based on *Brassica carinata* leaf tissue samples from two growing seasons with samples taken based on plant life stages. ⁴ Reference values based on 50 mature leaves without petioles taken throughout the season from rosette stage to pod set. Values taken from *Brassica napus* leaf tissue values from Bryson et al. [45].

During the rosette stage, differences were observed in total plant dry weights; however, when those values were compared to the leaf tissue values, the increase in Fe fertility did not result in an increase in tissue Fe concentrations (Table 3). Given the nutrient solutions were replaced weekly and the tested values for the solutions were within the target ranges, a potential contamination issue was unlikely. The lowest fertility concentration (0.0 μmol·L⁻¹) provided no Fe; thus, it seems likely that the limited plant biomass production resulted in an elevated concentration of Fe within the leaf tissue. Plants will contain trace amounts of micronutrients naturally, which are typically sourced from the seed reserves. This concentration effect may be a reflection of higher accumulation of leaf tissue Fe in the 0.0 μmol·L⁻¹ treatment when compared to the lower plant biomass. When the plants were provided with higher levels of Fe, it resulted in an increase in plant growth and thus a dilution of the Fe concentrations, which has been reported extensively in other crops [45]. Additionally, Brassicas are very effective at scavenging nutrients from the soil profile [50]. This scavenging of nutrients could have resulted in a higher Fe seed load, which was higher in concentration given the dilution effect discussed above.

Additionally, in a study conducted by Wu et al. [51], a half-strength Hoagland's solution was used to grow 111 different *Brassica napus* ascensions to explore the differences in accumulation of Zn, Fe, and Mn. They reported that different individuals accumulated a wide range of leaf tissue concentrations of 60.3–350.1 μg·g⁻¹ Fe even with a half-strength Hoagland's solution. The leaf tissue Fe values reported by Wu were much higher than our reported values. Given Wu's experiment used a half-strength Hoagland's solution for 14 days and certain Brassica ascensions accumulated leaf tissue values within our ranges, it may be that *B. carinata* has greater Fe use efficiency [50].

3.2.3. Bolting-Stage Fe Rates

Bolting plants varied in the distribution of their dry weights based on Fe fertility concentrations (Table 3). Leaf tissue Fe concentrations were similar except for the $63.0 \mu\text{mol}\cdot\text{L}^{-1}$ Fe concentration, which contained almost double the leaf tissue Fe concentration when compared to other rates (Table 3). Because of the limited statistical significance among the Fe levels, regression models for the plant dry weights and the leaf tissue concentrations provided little explanatory power (Table S2).

The lowest fertility rates in both the bolting and flowering stages contained lower concentrations of Fe than observed at the rosette stage. The lower Fe values could be the result of a dilution effect given the bolting stage plants weighed over 26 times greater than the smaller rosette stage plants (Table 3).

3.2.4. Flowering-Stage Fe Rates

Flowering plants did not differ significantly in dry weights regardless of Fe concentration. Leaf tissue Fe concentration only displayed statistical differences between the $63.0 \mu\text{mol}\cdot\text{L}^{-1}$ Fe concentration and all other concentrations except the $54.0 \mu\text{mol}\cdot\text{L}^{-1}$ concentration, which was statistically similar (Table 3). Except for the $72.0 \mu\text{mol}\cdot\text{L}^{-1}$ concentration, there was a quadratic trend of leaf tissue Fe accumulation with increasing fertility. Regression models from these confounding results only accounted for 25.0% (linear) and 30.0% (quadratic) of the variation when treating leaf tissue Fe as the dependent variable and Fe fertility concentration as the predictor (Table S2).

3.3. Copper

3.3.1. Cu Deficiency Symptomology

The visual impacts of Cu deficiency were not present even at the lowest fertility concentrations across all life stages. Despite the lack of visual deficiency symptoms, a strong impact occurred in the response of leaf tissue to Cu concentrations across all life stages. Based on comparisons with canola and *B. napus*, tissue concentrations at all stages were within the normal range, with the exception of the 0 Cu treatment at bolting.

3.3.2. Rosette-Stage Cu Rates

Rosette plants varied in dry weights based on Cu fertility concentration, but no discernable trend occurred as Cu concentrations increased (Table S3 and Table 4). The regression models resulted in no statistically significant results for either linear or quadratic models for the relationship between plant dry weight and Cu fertility (Table S3).

Despite the lack of a discernable trend within the plant dry weights, the leaf tissue Cu concentration exhibited an increasing trend in Cu with the exception of the $2.25 \mu\text{mol}\cdot\text{L}^{-1}$ Cu, which was slightly lower than the 1.50, 2.63, and $3.00 \mu\text{mol}\cdot\text{L}^{-1}$ concentrations (Table 4). The lowest Cu concentration (0.00) differed significantly from all other concentrations and was the lowest recorded value (Table 4). The quadratic regression model accounted for the most variability when treating leaf tissue Cu as the dependent variable and Cu fertility concentration as the predictor (Table 4, Table S3).

These results indicate that increasing Cu levels may not result in a consistent increase in plant dry weight at the rosette stage, despite an increase in accumulation of leaf tissue Cu levels. Among the Cu treatments, many growth metrics were maximized at lower fertility levels, indicating that *carinata* may require less Cu fertility than other Brassica crops [12].

Table 4. *Brassica carinata* plant dry weights (g) and leaf tissue concentration (mg·kg⁻¹) based on copper (Cu) fertility treatments.

Cu Fertility (μmol·L ⁻¹) ¹	0.00	0.75	1.50	2.25	2.63	3.0
Plant Dry Weight (g)						
Rosette	7.26 BCD ***	10.26 A ***	9.38 AB ***	6.63 CD ***	5.67 D ***	8.53 ABC ***
Bolting	22.89 A ***	46.56 B ***	37.22 BC ***	29.14 AB ***	33.51 ABC ***	31.51 AB ***
Flowering	27.54 AB ***	21.67 A ***	48.29 C ***	40.56 BC ***	37.63 BC ***	40.68 BC ***
Cu Leaf Tissue Nutrient Concentrations (mg·kg⁻¹)						
Rosette	2.75 A ***	5.91 B ***	7.85 C ***	6.06 B ***	7.63 C ***	8.03 C ***
Bolting	1.22 A ***	3.91 B ***	6.12 BC ***	7.98 C ***	6.62 C ***	7.57 C ***
Flowering	4.14 A **	7.88 AB **	8.96 B **	10.92 B **	9.52 B **	10.37 B **
Comparison Cu Leaf Tissue Values (mg·kg⁻¹)³						
	<i>Brassica carinata</i> ³			<i>Brassica napus</i> ⁴		
Rosette ³	1.9–3.2					
Bolting ³	3.4–3.6			4.0–25.0		
Flowering ³	2.3–3.2					

¹ Values indicate the adjusted fertility rate provided from a modified Hoagland's solution with all elements held constant except the adjusted microelement being studied [41]. ² *, **, or *** indicate statistically significant differences between sample means across a row based on *F*-test (proc GLM) at $p \leq 0.05$, $p \leq 0.01$, or $p \leq 0.001$, respectively. NS (not significant) indicates the *F*-test difference between sample means was $p > 0.05$. Values with the same letter indicate a lack of statistical significance, whereas values with different letters indicate statistically significant results. ³ Reference values from Seepaul et al. [6,14]. Values given are based on *Brassica carinata* leaf tissue samples from two growing seasons with samples taken based on plant life stages. ⁴ Reference values based on 50 mature leaves without petioles taken throughout the season from rosette stage to pod set. Values taken from *Brassica napus* leaf tissue values from Bryson et al. [45].

3.3.3. Bolting-Stage Cu Rates

Bolting plant dry weights modeled on a parabolic trend with the middle concentrations forming the vertex and the lowest and highest concentrations forming the tails, though the quadratic model interpreted only a low proportion of the data accurately (Table S3). Given the variability of the dry weights and the low statistical significance, the models presented should be used with only a small degree of certainty.

Leaf tissue Cu concentration exhibited an increasing trend with increases in Cu fertilization rate (Table 4). Leaf tissue Cu concentration was lowest at 0.0 μmol·L⁻¹ Cu and was statistically less than all other concentrations. The three highest concentrations (2.25, 2.63, and 3.00 μmol·L⁻¹ Cu) were all statistically similar (Table 4). The results observed at the bolting stage regarding plant dry weights indicate that optimization of leaf tissue Cu would be obtained when plant leaf tissue is at an average value of 7.39 mg·kg⁻¹ (Table 4). These results indicate that during times of rapid cell growth and expansion, the Cu requirements of the plant vary little from the Cu needs at the rosette stage.

This may be indicative of the role of Cu in plants. Most of the Cu contained within plants is used in the chloroplasts as plastocyanin [11]. The main role of this protein is to assist in the electron transport chain in the photosystem I complex. A study conducted with *Pisum sativum* plants had an 87.5% decrease in plastocyanin, which resulted in a decrease of photosynthetic electron transport from 100 to 19 (nmol·μmol⁻¹ chlorophyll) between leaf Cu fertility concentrations of 6.9 to 2.2 μmol·g⁻¹, respectively [52]. Additionally, this study reported a decrease in other Cu-related enzymes with a marked decrease in the activity of diamineoxidase, ascorbateoxidase, and CuZnSOD. Given most photosynthates are produced in the rosette and bolting stage, the data imply that the Cu-containing molecules within Brassicas will be most active during these stages [11,52,53]. After the initiation

of flowering, the sources and sinks within Brassicas are altered significantly [53]. Thus, the limiting factors within the flowering stage would be more regulated based on other predictors such as photosynthates and Cu fertility.

3.3.4. Flowering-Stage Cu Rates

Flowering plant models indicated a general increasing trend in dry weights with regard to Cu fertility with the exception of the 0.75 and 1.50 $\mu\text{mol}\cdot\text{L}^{-1}$ Cu, which displayed upper and lower outliers of the general trend, respectively (Table S3). Leaf tissue Cu concentration also exhibited a general increasing trend as Cu concentrations increased except for the 2.63 $\mu\text{mol}\cdot\text{L}^{-1}$ concentration (Table 4). Leaf tissue Cu concentrations were statistically different between the lowest concentration and the remaining concentrations apart from the 0.75 concentration, which was statistically similar (Table 4). A strong plateau was observed within this dataset, indicating optimal uptake for plant leaf tissue Cu may be at 1.50 $\mu\text{mol}\cdot\text{L}^{-1}$ Cu (Table 4). These results also indicate that Cu may be less regulating in the flowering stage than in the rosette stage.

3.4. Zinc (Zn)

Limited symptomology occurred with Zn, which manifested as a slight decrease in bolting vigor and branching when compared to the controls. After the initiation of the reproductive phase, the sources and sinks changed within the plants, and growth slowed given *carinata* is a determinate flowering plant.

3.4.1. Zn Deficiency Symptomology

Deficiency symptoms of Zn were only present with 0.00 $\mu\text{mol}\cdot\text{L}^{-1}$ Zn. Zinc deficiency symptoms were observed later in *carinata* growth compared to other nutrients. Zinc-deficient plants appeared large and healthy and displayed only subtle signs of nutrient stress (Figure S9). Symptomology appeared on the mid to upper foliage as a slight paling of the leaf margin and gall-like structures (Figure S10). As symptoms advanced, the slight yellowing or paling progressed to a slight purple coloration on the margin of the leaves (Figure S10).

3.4.2. Rosette-Stage Zn Rates

Rosette plants exhibited no discernable pattern or trend among Zn treatments, with total plant dry weight varying greatly as Zn concentrations increased (Table S4 and Table 5). The highest Zn concentration (3.00 $\mu\text{mol}\cdot\text{L}^{-1}$) had the greatest dry weight and was statistically significant from the other concentrations except for the 2.25 $\mu\text{mol}\cdot\text{L}^{-1}$ concentration (Table 5). Leaf tissue Zn levels increased until the 2.25 $\mu\text{mol}\cdot\text{L}^{-1}$ Zn concentration, after which point all other concentrations were statistically similar (Table 5). Both a linear and quadratic regression model accounted for little variance within the Zn leaf tissue values (Table S4). However, there was a strong quadratic trend regarding increasing Zn concentration and plant biomass production. The plateau in leaf tissue at 2.25 $\mu\text{mol}\cdot\text{L}^{-1}$ Zn indicates a greater Zn fertility requirement for *B. carinata* in the rosette stage. Leaf tissue Zn concentrations in *carinata* that were below the suggested normal tissue concentrations of canola and *B. napus* were found when grown solution concentrations were <2.25 $\mu\text{mol}\cdot\text{L}^{-1}$.

The differences observed in Zn uptake in the rosette stage could be a result of the growth stage and the physiological function of Zn within the plant. The major role of Zn within plant cells and functions are mainly enzymatic activity [54,55] and regulation of genetic expression and replication [26].

There are also indications that when Zn levels are elevated, the phloem could absorb and store Zn within the plant [56]. This storage ability in Zn concentrations may have resulted in an unexpectedly higher value of Zn within the leaf tissue during the rosette stage.

Table 5. *Brassica carinata* plant dry weights (g) and leaf tissue concentration ($\text{mg}\cdot\text{kg}^{-1}$) based on zinc (Zn) fertility treatments.

Zn Fertility ($\mu\text{mol}\cdot\text{L}^{-1}$) ^{1,2}	0.0	0.75	1.50	2.25	2.63	3.0
Plant Dry Weight (g)						
Rosette	5.84 A ***	5.72 A ***	6.74 AB ***	7.46 BC ***	5.61 A ***	8.53 C ***
Bolting	32.21 A **	15.42 B **	24.96 AB **	32.91 A **	16.06 B **	31.51 A **
Flowering	34.15 AB ***	22.11 B ***	37.40 AB ***	38.03 AB ***	36.80 AB ***	40.68 AB ***
Zn Leaf Tissue Nutrient Concentrations ($\text{mg}\cdot\text{kg}^{-1}$)						
Rosette	14.66 A ***	13.18 A ***	19.07 B ***	23.22 C ***	21.02 BC ***	22.65 C ***
Bolting	9.17 A ***	27.47 B ***	34.92 B ***	39.61 B ***	39.87 B ***	29.10 B ***
Flowering	15.50 A *	33.98 B *	42.26 B *	43.41 B *	43.50 B *	43.43 B *
Comparison Zn Leaf Tissue Values ($\text{mg}\cdot\text{kg}^{-1}$)³						
	<i>Brassica carinata</i> ³			<i>Brassica napus</i> ⁴		
Rosette ³	21.9–25.3					
Bolting ³	20.9–25.7			22.0–49.0		
Flowering ³	22.7–28.0					

¹ Values indicate the adjusted fertility rate provided from a modified Hoagland's solution with all elements held constant except the adjusted microelement being studied [41]. ² *, **, or *** indicate statistically significant differences between sample means across a row based on *F*-test (proc GLM) at $p \leq 0.05$, $p \leq 0.01$, or $p \leq 0.001$, respectively. NS (not significant) indicates the *F*-test difference between sample means was $p > 0.05$. Values with the same letter indicate a lack of statistical significance, whereas values with different letters indicate statistically significant results. ³ Reference values from Seepaul et al. [6,14]. Values given are based on *Brassica carinata* leaf tissue samples from two growing seasons with samples taken based on plant life stages. ⁴ Reference values based on 50 mature leaves without petioles taken throughout the season from rosette stage to pod set. Values taken from *Brassica napus* leaf tissue values from Bryson et al. [45].

3.4.3. Bolting-Stage Zn Rates

Bolting plants resulted in no discernable trends among Zn concentrations. The dry weights varied greatly, with the lowest dry weight occurring at $0.75 \mu\text{mol}\cdot\text{L}^{-1}$ concentration and being statistically similar to 1.50 and $2.63 \mu\text{mol}\cdot\text{L}^{-1}$ Zn levels (Table 5). This is not surprising, given the extreme variability in bolting times observed within the Zn treatments. Zinc requirements may be lower in the bolting stage, given the plateau occurred at a lower Zn concentration when compared to the rosette stage. Leaf tissue Zn levels exhibited an increasing trend until $0.75 \mu\text{mol}\cdot\text{L}^{-1}$ Zn concentration, after which leaf tissue values plateaued (Table 5).

At the rosette stage, *B. carinata* has a very compact growth habit [6]. When bolting occurs, a very rapid vertical flower spikelet and branching architecture result. Additionally, Brassicas can vary greatly in their bolting vigor and timing [57]. Thus, the lower plateau observed at the concentrations above $0.75 \mu\text{mol}\cdot\text{L}^{-1}$ Zn may indicate a dilution effect given biomass increased greatly during the bolting stage or simply differences in bolting time among plants. The lack of a statistically significant trend regarding dry weights may indicate that factors other than nutrient stress play a larger regulating role in bolting *B. carinata*.

3.4.4. Flowering-Stage Zn Rates

Flowering plant dry weights did not result in a plateau. The lowest dry weight occurred at $0.75 \mu\text{mol}\cdot\text{L}^{-1}$ Zn. Leaf tissue Zn concentration mirrored the plateau at $0.75 \mu\text{mol}\cdot\text{L}^{-1}$ Zn regarding leaf tissue Zn at the bolting stage (Table 5). Leaf tissue Zn concentration was lowest at $0.00 \mu\text{mol}\cdot\text{L}^{-1}$, which was statistically different from all other concentrations (Table 5).

While plant dry weights did not display a clear trend, the explanatory power of the Zn fertility on leaf tissue concentration was apparent. The plateau observed at the $0.75 \mu\text{mol}\cdot\text{L}^{-1}$ Zn for both the bolting and flowering stage may be due to the role of Zn in many enzymatic functions within the plant. Work conducted by Cakmak and Marschner [30] reported when cotton plants were subjected to Zn deprivation conditions, the activity of superoxide dismutase (SOD) within the roots decreased, and a resultant increase in superoxide oxygen radicals occurred. Additional work by the above authors also reported a decrease in nicotinamide adenine dinucleotide phosphate (NADPH) production of oxides, plasma membrane permeability, and differences in nutrient uptake and partitioning under Zn-deficient conditions [30,58,59]. Given that many of the above impacts are on enzymatic driven processes, a lower concentration of Zn ($0.75 \mu\text{mol}\cdot\text{L}^{-1}$) could indicate enzymatic function can be optimized at a lower Zn concentration.

3.5. Molybdenum (Mo)

3.5.1. Mo Deficiency Symptoms

Visual deficiency symptoms of Mo did not manifest at any concentration or stage of development despite significant differences in leaf tissue levels. Molybdenum, overall, resulted in a linear increase in plant biomass regarding concentration at the rosette stage, and no discernable trends occurred at the bolting or flowering stages. Regarding leaf tissue Mo concentration, however, a strong linear increase was found between increasing Mo concentrations and Mo leaf tissue concentrations in the rosette and bolting stages (Table S5). However, in the flowering stage, the model resulted in a plateau regarding Mo accumulation. Note that all plant tissue Mo concentrations here were within or exceeded the normal concentration range reported for *B. napus*.

3.5.2. Rosette-Stage Mo Rates

Rosette plants varied in the distribution of their dry weights based on Mo fertility concentrations. Total plant dry weight, when modeled against Mo concentrations, displayed no discernable trend (Table 6). Leaf tissue Mo levels were similar for all treatments with only the highest concentration resulting in higher Mo concentrations in leaf tissue as compared with $0.0 \mu\text{mol}\cdot\text{L}^{-1}$ Mo (Table 6).

Table 6. *Brassica carinata* plant dry weights (g) and leaf tissue concentration ($\text{mg}\cdot\text{kg}^{-1}$) based on molybdenum (Mo) fertility treatments.

Mo Fertility ($\mu\text{mol}\cdot\text{L}^{-1}$) ^{1,2}	0.0	0.025	0.050	0.075	0.088	0.10
Plant Dry Weight (g)						
Rosette	5.62 A ***	7.59 AB ***	7.06 AB ***	6.54 AB ***	12.18 C ***	8.53 B ***
Bolting	42.78 A **	19.99 B **	33.17 AB **	30.74 AB **	30.02 AB **	31.51 AB **
Flowering	50.69 A NS	30.51 A NS	44.26 A NS	38.00 A NS	55.52 A NS	40.68 A NS
Mo Leaf Tissue Nutrient Concentrations ($\text{mg}\cdot\text{kg}^{-1}$)						
Rosette	0.39 A ***	0.31 A ***	1.61 A ***	1.21 A ***	1.03 A ***	14.53 B ***
Bolting	0.31 A ***	1.17 AB ***	1.28 AB ***	1.93 BC ***	2.21 BC ***	3.15 C ***
Flowering	0.80 A ***	1.59 AB ***	2.89 C ***	3.00 C ***	3.23 C ***	2.42 C ***

Table 6. Cont.

Mo Fertility ($\mu\text{mol}\cdot\text{L}^{-1}$) ^{1,2}	0.0	0.025	0.050	0.075	0.088	0.10
Comparison Mo Leaf Tissue Values ($\text{mg}\cdot\text{kg}^{-1}$) ³						
	<i>Brassica carinata</i> ³			<i>Brassica napus</i> ⁴		
Rosette ³	N/A ³					
Bolting ³	N/A ³			0.25–0.60		
Flowering ³	N/A ³					

¹ Values indicate the adjusted fertility rate provided from a modified Hoagland's solution with all elements held constant except the adjusted microelement being studied [41]. ² *, **, or *** indicate statistically significant differences between sample means across a row based on *F*-test (proc GLM) at $p \leq 0.05$, $p \leq 0.01$, or $p \leq 0.001$, respectively. NS (not significant) indicates the *F*-test difference between sample means was $p > 0.05$. Values with the same letter indicate a lack of statistical significance, whereas values with different letters indicate statistically significant results. ³ Reference values from Seepaul et al. [6,14]. Values given are based on *Brassica carinata* leaf tissue samples from two growing seasons with samples taken based on plant life stages. ⁴ Reference values based on 50 mature leaves without petioles taken throughout the season from rosette stage to pod set. Values taken from *Brassica napus* leaf tissue values from Bryson et al. [45].

3.5.3. Bolting-Stage Mo Rates

Bolting plants varied in the distribution of their dry weights and leaf tissue Mo based on fertility concentrations (Table 6). Leaf tissue Mo concentration exhibited an increasing trend as concentration increased (Table 6). Leaf tissue Mo concentration increased with the lowest three concentrations (0.0, 0.025, and 0.05 $\mu\text{mol}\cdot\text{L}^{-1}$ Mo) being statistically similar (Table 6). The next two highest concentrations (0.075 and 0.088 $\mu\text{mol}\cdot\text{L}^{-1}$ Mo) were statistically similar to each other but were significantly higher in Mo leaf tissue levels when compared to the 0.00 $\mu\text{mol}\cdot\text{L}^{-1}$ Mo. The highest Mo concentration (0.10 $\mu\text{mol}\cdot\text{L}^{-1}$) resulted in the highest Mo levels within the leaf tissue and were statistically significant from only the three lowest concentrations (Table 6).

3.5.4. Flowering-Stage Mo Rates

In the flowering plants, there was no significant difference in dry weights among Mo concentrations (Table S5 and Table 6). Despite a lack of statistical significance in the plant dry weights, leaf tissue Mo concentration resulted in an increasing trend as Mo concentrations increased up to the 0.05 $\mu\text{mol}\cdot\text{L}^{-1}$ Mo treatment, above which all leaf tissue values were statistically similar (Table 6). The similarity of the plant biomass production among Mo concentrations and life stages may indicate that only a minimal threshold of Mo is required to benefit *B. carinata*. It has been reported that Mo mainly provides benefits to nodulating and leguminous crops despite also being used in the xanthine oxidase/dehydrogenase reaction in plants [60]. While other crops receive great benefit from Mo, the extremely low concentrations required by the plant often dictate that Mo will be adequate from ambient sources within the soil.

3.6. Manganese (Mn)

Results varied by life stages and across Mn concentrations. Very little differences occurred among the dry weights for different growth stages and concentrations. Except for the 0 Mn treatment, and plant tissues had Mn concentrations within or exceeding the normal ranges suggested for canola and *B. napus*.

3.6.1. Mn Deficiency Symptomatology

Deficiency symptoms of Mn were observed later in growth trials than most other nutrients. Manganese is an immobile element and thus cannot translocate from the lower foliage to the upper foliage, and deficiency symptoms will manifest in the newer developing leaves. Plants were in the advanced stages of vegetative growth, exhibiting a general paling of the entire plant when compared with the control (Figure S11). This paling was more pronounced on the mid and upper foliage (Figure S12).

3.6.2. Rosette-Stage Mn Rates

Rosette plants varied in the distribution of their dry weights based on Mn fertility concentrations. Total plant dry weight exhibited no distinct trend with the increase of Mn fertility (Table 7). Leaf tissue Mn concentrations displayed an increasing trend as Mn fertility increased. The lowest leaf tissue Mn values occurred at the 0.0 $\mu\text{mol}\cdot\text{L}^{-1}$ Mn concentration and were statistically less than all other rates (Table 7). The highest Mn values were observed with 15.75 $\mu\text{mol}\cdot\text{L}^{-1}$ Mn and were statistically similar to the 13.50 $\mu\text{mol}\cdot\text{L}^{-1}$ Mn and significantly higher than the other Mn rates (Table 7). Regression models indicated that a quadratic model accounted for more variability in the dataset when Mn fertility concentration was treated as the independent variable (Table S6). The decrease in Mn leaf tissue concentrations at 18.0 $\mu\text{mol}\cdot\text{L}^{-1}$ Mn may indicate that a sigmoidal model is present with the vertex being at the 13.5 and 15.75 $\mu\text{mol}\cdot\text{L}^{-1}$ Mn treatments (Table 7).

Table 7. *Brassica carinata* plant dry weights (g) and leaf tissue concentration ($\text{mg}\cdot\text{kg}^{-1}$) based on manganese (Mn) fertility treatments.

Mn Fertility Rate ($\mu\text{mol}\cdot\text{L}^{-1}$) ^{1,2}	0.0	4.50	9.0	13.50	15.75	18.0
Plant Dry Weight (g)						
Rosette	6.29 CD ***	8.71 AB ***	10.65 A ***	5.81 D ***	6.41 BCD ***	8.53 ABC ***
Bolting	23.34 A NS	29.85 A NS	33.30 A NS	24.93 A NS	25.94 A NS	31.51 A NS
Flowering	24.33 A NS	49.08 A NS	51.16 A NS	30.45 A NS	39.00 A NS	40.68 A NS
Mn Leaf Tissue Nutrient Concentrations ($\text{mg}\cdot\text{kg}^{-1}$)						
Rosette	14.70 A ***	74.31 B ***	112.11 C ***	149.36 D ***	155.93 D ***	103.25 C ***
Bolting	8.77 A ***	65.21 B ***	117.03 C ***	149.87 C ***	137.09 C ***	161.63 C ***
Flowering	6.90 A ***	61.56 B ***	105.20 C ***	132.17 CD ***	139.14 CD ***	145.70 D ***
Comparison Mn Leaf Tissue Values ($\text{mg}\cdot\text{kg}^{-1}$)³						
	<i>Brassica carinata</i> ³			<i>Brassica napus</i> ⁴		
Rosette	17.1–22.6			25.0–250.0		
Bolting	9.5–17.1					
Flowering	11.6–18.7					

¹ Values indicate the adjusted fertility rate provided from a modified Hoagland's solution with all elements held constant except the adjusted microelement being studied [41]. ² *, **, or *** indicate statistically significant differences between sample means across a row based on *F*-test (proc GLM) at $p \leq 0.05$, $p \leq 0.01$, or $p \leq 0.001$, respectively. NS (not significant) indicates the *F*-test difference between sample means was $p > 0.05$. Values with the same letter indicate a lack of statistical significance, whereas values with different letters indicate statistically significant results. ³ Reference values from Seepaul et al. [6,14]. Values given are based on *Brassica carinata* leaf tissue samples from two growing seasons with samples taken based on plant life stages. ⁴ Reference values based on 50 mature leaves without petioles taken throughout the season from rosette stage to pod set. Values taken from *Brassica napus* leaf tissue values from Bryson et al. [45].

3.6.3. Bolting-Stage Mn Rates

Bolting plants displayed no differences in dry weights among Mn concentrations. However, leaf tissue Mn concentration exhibited an increasing trend as Mn fertility increased (Table S6 and Table 7). Leaf tissue Mn concentration was lowest at 0.0 $\mu\text{mol}\cdot\text{L}^{-1}$ Mn and was statistically smaller than all other concentrations. The second-lowest Mn leaf tissue later occurred at 4.50 $\mu\text{mol}\cdot\text{L}^{-1}$ Mn and was statistically smaller than the higher concentrations. The next four concentrations (9.00, 13.50, 15.75, and 18.00 $\mu\text{mol}\cdot\text{L}^{-1}$ Mn) were all statistically similar, indicating a plateau in leaf tissue Mn accumulation (Table 7). A polynomial regression model accounted for 88% of the variability of leaf tissue Mn concentration when Mn fertility concentration was treated as the independent variable (Table S6).

These results may indicate that at earlier stages (rosette) of growth, Mn is more important to the plant. The low r^2 value (0.075) of the polynomial regression of plant biomass at the bolting stage may indicate that other factors regulate bolting more strongly than Mn concentrations or that the concentrations studied were in a range that was not adequate to test the importance of Mn (Table S6). This makes sense given the role of Mn in the plant as the manganese-protein in photosystem II (PS II) as well as in the superoxide dismutase (MnSOD) [61]. This indicates that Mn may have a greater impact on photosynthesis and the resultant photosynthates produced in the plant rather than directly regulating plant cellular growth and expansion.

3.6.4. Flowering-Stage Mn Rates

Flowering plant data dry weights were similar for all Mn rates at flowering (Table S6 and Table 7). Leaf tissue Mn increased with increasing fertility concentrations, with the lowest fertility treatment ($0.0 \mu\text{mol}\cdot\text{L}^{-1}$ Mn) leaf tissue Mn being statistically lower compared to the remaining treatments. The $4.50 \mu\text{mol}\cdot\text{L}^{-1}$ Mn treatment had Mn tissue values that were $8.9\times$ higher than $0.00 \mu\text{mol}\cdot\text{L}^{-1}$ Mn and were significantly smaller than the upper four ($9.0, 13.50, 15.75,$ and $18.0 \mu\text{mol}\cdot\text{L}^{-1}$ Mn) concentrations (Table 7). The highest Mn concentration ($18.0 \mu\text{mol}\cdot\text{L}^{-1}$ Mn) resulted in the leaf tissue of the highest concentration and was statistically higher when compared to the lower three concentrations ($9.00, 13.50,$ and $15.75 \mu\text{mol}\cdot\text{L}^{-1}$ Mn), but not the upper concentrations of 13.50 and $15.75 \mu\text{mol}\cdot\text{L}^{-1}$ Mn (Table 7). The quadratic regression model accounted for 91% of the variability of leaf tissue Mn concentration when Mn fertility concentration was treated as the independent variable (Table S6).

The higher Mn leaf accumulation may indicate that as the developing sinks of the floral and subsequent reproductive structures increase in demand, more Mn resources are accumulated and used by the plants. This would make sense, given Mn's role in the photosynthetic O_2 evolution in PS II and the role of Mn in the lignin content of plants [62,63]. The impacts of the higher Mn rates would ensure that the photosynthate resources produced by PS II would be present in higher concentrations for the developing reproductive sinks.

4. Conclusions

Different levels of micronutrients are required at different optimal concentrations over the life stages of *B. carinata*. The biomass production optimization and leaf tissue concentrations can be used as guidelines to help inform other research regarding field fertility, uptake and partitioning, and life-stage-based fertility studies. Given B, Mn, and Cu showed the greatest concentration increase differences between the lower fertility rates tested (0.0 and 25.0%), this may indicate that the rates tested may have needed an increased number of lower datapoints. Thus, for some life stages, the fertility concentrations may have needed to be expanded at the lower end. This would have allowed for a more gradual increase in the plateau curve. For each of the micronutrients tested, each of the Tables 2, 3 and 5–7 compare tissue values to known *B. carinata* and *B. napus* tissue values from published literature, as well as providing trends in leaf tissue mineral accumulation and biomass production based on life stage.

These results indicated that B fertility had the greatest impact on plant biomass and production, given the lowest rate ($0.0 \mu\text{mol}\cdot\text{L}^{-1}$) did not produce any flowers or siliques. Iron fertility concentrations resulted in a dilution effect that skewed the results slightly. The dilution effect has been reported extensively in other crops [45]. For Cu fertility, despite the lack of visual symptoms, leaf tissue accumulation plateaus were observed in the bolting and flowering stages, indicating Cu may be more important in the rosette stage. Zinc fertility displayed mixed results regarding increasing fertility and plant biomass production. However, plateaus (occurring at lower fertility concentrations) were observed in both the bolting and flowering stages. Molybdenum fertility concentrations plateaued early for leaf tissue accumulation for the bolting and flowering stages. Finally, Mn leaf

tissue accumulation was maximized between 9.0 and 15.75 $\mu\text{mol}\cdot\text{L}^{-1}$ depending on life stage. These results indicate strong nutrient use and uptake for micronutrients in *B. carinata* leaf tissue. More research is needed to elucidate the exact uptake and partitioning of these microelements to determine optimal fertility concentrations.

Supplementary Materials: The following are available online at <https://www.mdpi.com/2077-0472/11/3/221/s1>, Figure S1: Categorization of the growth stages of *Brassica carinata* based on life stage and development from germination to senescence developed by the South East Partnership for Advanced Renewables from *Carinata* (SPARC), Figure S2: Boron deficiency in *Brassica carinata* first manifested as a general distortion of the upper leaves. Note that the distortion resulted in folding of the leaves rather than as curling, cupping, or withering of the leaf surface. This folding was concentrated along the margin and midrib similar to the leaf was being folded in half lengthwise, Figure S3: As boron deficiency symptomatology in *Brassica carinata* progressed, the folding became more severe, especially on new foliage. The newest foliage appeared rolled on itself like a tube of paper. This rolling is different than the cupping of the leaves observed in calcium deficient leaves because the whole leaf blade curls from the midrib to the margin whereas calcium deficiency results in only the leaf margin curling in and downward, Figure S4: As symptoms of boron deficiency progressed in *Brassica carinata*, the new leaves exhibited cracking along the midrib and petiole. This leaf curling along with the cracking are classical boron deficiency symptoms, Figure S5: In the advanced stages of boron deficiency, the apical meristem becomes necrotic and eventually dies in *Brassica carinata*. This results in the proliferation of axillary shoots as the plant continues to grow, Figure S6: Boron deficiency in *Brassica carinata* will eventually result in the death of the apical meristem. This sudden loss of apical dominance results in the axillary shoot growth, resulting in numerous axillary shoots. Note the dense cluster of side shoots around the dead growing tip, Figure S7: Iron deficiency symptoms in *Brassica carinata* were present in the rosette stage for *Brassica carinata* and were quite severe in the lowest ($0.0 \mu\text{mol Fe}\cdot\text{L}^{-1}$) fertility treatment resulting in newer and developing leaves which had interveinal chlorosis, Figure S8: Symptoms of iron deficiency in *Brassica carinata* were present at the lowest fertility treatment ($0.0 \mu\text{mol}\cdot\text{L}^{-1}$) at both the flowering (top) and pod set (bottom) stages, Figure S9: Initially, this *Brassica carinata* plant appeared healthy and vigorous. As the plant grew out of its rosette phase and into the beginning phases of elongation/bolting before zinc deficiency symptoms began to appear, Figure S10, The beginning stages of zinc deficiency in *Brassica carinata* appeared very late in the experiment as a marginal paleness and purpling of the leaf margin especially of the leaf tip. Also note the gall like structures on the leaf surface. When diagnosing Zn deficiency these two symptoms are unique symptomologies, Figure S11: The *Brassica carinata* plant on the left received all its essential macro and micronutrients while the plant on the right is exhibiting manganese deficiency symptoms. Note specifically the pale coloration of the plant especially along the upper mature leaves, Figure S12: Manganese deficient *Brassica carinata* plants resulted in a pale coloration (right leaf, A and B) compared with non-deficient leaf (left leaf A, B). The coloration was more developed in the upper (A) and mid (B) foliage of the plant. Table S1: Regression models for linear and quadratic *Brassica carinata* plant dry weights (g) and leaf tissue nutrient concentrations ($\text{mg}\cdot\text{kg}^{-1}$) based on boron (B) fertility treatments. Table S2: Regression models for linear and quadratic *Brassica carinata* plant dry weights (g) and leaf tissue nutrient concentrations ($\text{mg}\cdot\text{kg}^{-1}$) based on iron (Fe) fertility treatments. Table S3: Regression models for linear and quadratic *Brassica carinata* plant dry weights (g) and leaf tissue nutrient concentrations ($\text{mg}\cdot\text{kg}^{-1}$) based on copper (Cu) fertility treatments. Table S4: Regression models for linear and quadratic *Brassica carinata* plant dry weights (g) and leaf tissue nutrient concentrations ($\text{mg}\cdot\text{kg}^{-1}$) based on zinc (Zn) fertility treatments. Table S5: Regression models for linear and quadratic *Brassica carinata* plant dry weights (g) and leaf tissue nutrient concentrations ($\text{mg}\cdot\text{kg}^{-1}$) based on molybdenum (Mo) fertility treatments. Table S6: Regression models for linear and quadratic *Brassica carinata* plant dry weights (g) and leaf tissue nutrient concentrations ($\text{mg}\cdot\text{kg}^{-1}$) based on manganese (Mn) fertility treatments.

Author Contributions: Conceptualization, P.C., A.P., C.R.C., R.G.L., R.P., and B.E.W.; methodology, P.C., P.V., M.D., G.B., A.P., C.R.C., R.P., and B.E.W.; software, P.C. and B.E.W.; validation, P.C., R.P., and B.E.W.; formal analysis, P.C., M.D., A.P., R.G.L., R.P., and B.E.W.; investigation, P.C., P.V., M.D., G.B., R.P., and B.E.W.; resources, A.P., C.R.C., R.G.L., and B.E.W.; data curation, P.C., P.V., M.D., G.B., R.P., and B.E.W.; writing—original draft preparation, P.C., P.V., A.P., R.P., and B.E.W.; writing—review and editing, P.C., P.V., A.P., C.R.C., R.G.L., R.P., and B.E.W.; visualization, P.C.; supervision, P.C., P.V., M.D., G.B., R.P., and B.E.W.; project administration, P.C., P.V., M.D., G.B., A.P., R.P., and B.E.W.; funding acquisition, A.P., C.R.C., R.G.L., and B.E.W. All authors have read and agreed to the published version of the manuscript.

Funding: This material is based on work that is supported by the National Institute of Food and Agriculture, USDA, under award number 2016-1123. Any opinions, findings, conclusions, or recommendations expressed in this publication are those of the author(s) and do not necessarily reflect the view of the U.S. Department of Agriculture.

Institutional Review Board Statement: Not applicable.

Informed Consent Statement: Not applicable.

Data Availability Statement: Not applicable.

Conflicts of Interest: The authors declare no conflict of interest.

References

- Govardhan, G.; Satheesh, S.K.; Nanjundiah, R.; Moorthy, K.K.; Babu, S.S. Possible climatic implications of high-altitude black carbon emissions. *Atmos. Chem. Phys. Discuss.* **2017**, *17*, 9623–9644. [CrossRef]
- Satheesh, S.K. High Altitude emissions of black carbon aerosols: Potential climate implications. *AGUFM* **2017**, *2017*, U21D-01.
- Craig, H. The natural distribution of radiocarbon and the exchange time of carbon dioxide between atmosphere and sea. *Tellus* **1957**, *9*, 1–7. [CrossRef]
- Friend, A.D.; Lucht, W.; Rademacher, T.T.; Keribin, R.; Betts, R.; Cadule, P.; Ciais, P.; Clark, D.B.; Dankers, R.; Falloon, P.D.; et al. Carbon residence time dominates uncertainty in terrestrial vegetation responses to future climate and atmospheric CO₂. In Proceedings of the National Academy of Sciences, Postdam, Germany, 4 March 2014; Volume 111, pp. 3280–3285.
- U.S. Energy Information Administration. Monthly Energy Review. 2016. Available online: <http://www.eia.gov/totalenergy/data/monthly/pdf/mer.pdf> (accessed on 8 November 2016).
- Seepaul, R.; George, S.; Wright, D.L. Comparative response of Brassica carinata and B. napus vegetative growth, development and photosynthesis to nitrogen nutrition. *Ind. Crop. Prod.* **2016**, *94*, 872–883. [CrossRef]
- United States Federal Aviation Administration; Pratt & Whitney. *Evaluation of ARA Catalytic Hydrothermolysis (CH) Fuel. Continuous Lower Energy, Emissions and Noise (CLEEN) Program*; Federal Aviation Administration: Washington, DC, USA, 2014.
- Fritsche, U.R.; Sims, R.E.H.; Monti, A. Direct and indirect land-use competition issues for energy crops and their sustainable production—An overview. *Biofuels Bioprod. Biorefining* **2010**, *4*, 692–704. [CrossRef]
- Christ, B.; Bartels, W.-L.; Broughton, D.; Seepaul, R.; Geller, D. In pursuit of a homegrown biofuel: Navigating systems of partnership, stakeholder knowledge, and adoption of Brassica carinata in the Southeast United States. *Energy Res. Soc. Sci.* **2020**, *70*. [CrossRef]
- Gesch, R.W.; Isbell, T.A.; Oblath, E.A.; Allen, B.L.; Archer, D.W.; Brown, J.; Hatfield, J.L.; Jabro, J.D.; Kiniry, J.R.; Long, D.S.; et al. Comparison of several Brassica species in the north central US for potential jet fuel feedstock. *Industrial crops and products. Ind. Crop. Prod.* **2015**, *75*, 2–7. [CrossRef]
- Marschner, H. *Marschner's Mineral Nutrition of Higher Plants*, 2nd ed.; Academic Press Inc.: San Diego, CA, USA, 1988.
- Gibson, J.L.; Nelson, P.V.; Pitchay, D.S.; Whipker, B.E. Identifying nutrient deficiencies of bedding plants. NC. State university floriculture research. *Florex* **2001**, *4*, 1–4.
- Grant, C.A.; Bailey, L.D. Fertility management in canola production. *Can. J. Plant Sci.* **1993**, *73*, 651–670. [CrossRef]
- Seepaul, R.; Small, I.M.; Marois, J.; George, S.; Wright, D.L. Brassica carinata and Brassica napus Growth, Nitrogen Use, Seed, and Oil Productivity Constrained by Post-Bolting Nitrogen Deficiency. *Crop. Sci.* **2019**, *59*, 2720–2732. [CrossRef]
- Harper, F.R.; Berkenkamp, B. Revised Growth-stage key for Brassica campestris and B. napus. *Can. J. Plant Sci.* **1975**, *55*, 657–658. [CrossRef]
- Matoh, T.B. Plant nutrition and cell wall development. In *Plant Nutrient Acquisition*; Ae, N., Arihara, J., Okada, K., Srinivasan, A., Eds.; Springer: Tokyo, Japan, 2001; pp. 227–250.
- Chebli, Y.; Geitmann, A. Cellular growth in plants requires regulation of cell wall biochemistry. *Curr. Opin. Cell Biol.* **2017**, *44*, 28–35. [CrossRef] [PubMed]
- Ma, B.-L.; Biswas, D.K.; Herath, A.W.; Whalen, J.K.; Ruan, S.Q.; Caldwell, C.; Earl, H.; Vanasse, A.; Scott, P.; Smith, D.L. Growth, yield, and yield components of canola as affected by nitrogen, sulfur, and boron application. *J. Plant Nutr. Soil Sci.* **2015**, *178*, 658–670. [CrossRef]

19. Yang, M.; Shi, L.; Xu, F.-S.; Lu, J.-W.; Wang, Y.-H. Effects of B, Mo, Zn, and Their Interactions on Seed Yield of Rapeseed (*Brassica napus* L.). *Pedosphere* **2009**, *19*, 53–59. [[CrossRef](#)]
20. Gardner, F.P.; Pearce, R.B.; Mitchell, R.L. *Physiology of Crop Plants*; Iowa State University Press: Ames, IA, USA, 2017.
21. Shetty, A.S.; Miller, G.W. Influence of Fe chlorosis on pigment and protein metabolism in leaves of *Nicotiana tabacum* L. *Plant Psychol.* **1966**, *41*, 415–421.
22. Terry, N.; Abadia, J. Function of Fe in chloroplasts. *J. Plant Nutr.* **1986**, *9*, 609–646. [[CrossRef](#)]
23. Rutherford, A.W. Photosystem II, the water-splitting enzyme. *Trends Biochem. Sci.* **1989**, *14*, 227–232. [[CrossRef](#)]
24. Fei, D.I.; Wang, X.F.; Shi, Q.H.; Wang, M.L.; Yang, F.J.; Gao, Q.H. Exogenous nitric oxide alleviated the inhibition of photosynthesis and antioxidant enzyme activities in Fe-deficient Chinese cabbage (*Brassica chinensis* L.). *Agric. Sci. China* **2008**, *7*, 168–179.
25. Hopmans, P. Stem deformity in *Pinus radiata* plantations in south-eastern Australia. *Plant Soil* **1990**, *122*, 97–104. [[CrossRef](#)]
26. Coleman, J.E. Zn proteins: Enzymes, storage proteins, transcription factors, and replication proteins. *Ann. Rev. Biochem.* **1992**, *61*, 897–946. [[CrossRef](#)]
27. Moore, P.A., Jr.; Patrick, W.H., Jr. Effect of Zn deficiency on alcohol dehydrogenase activity and nutrient uptake in rice. *Agron J.* **1988**, *80*, 882–885. [[CrossRef](#)]
28. Sandmann, G.; Boger, P. Enzymological function of heavy metals and their role in electron transfer processes of plants. In *Inorganic Plant Nutrition Encyclopedia of Plant Physiology, New Series*; Lauchli, A., Bielecki, R.L., Eds.; Springer: Bertin, Germany, 1983; Volume 15B, pp. 563–596.
29. O'sullivan, M. Aldolase activity in plants as an indicator of Zn deficiency. *J. Sci. Food Agric.* **1970**, *21*, 607–609. [[CrossRef](#)]
30. Cakmak, I.; Marschner, H. Enhanced superoxide radical production in roots of Zn-deficient plants. *J. Exp. Bot.* **1988**, *39*, 1449–1460. [[CrossRef](#)]
31. Akmak, I.; Marschner, H. Zinc-dependent changes in ESR signals, NADPH oxidase and plasma membrane permeability in cotton roots. *Physiol. Plant.* **1988**, *73*, 182–186.
32. Agarwala, S.C.; Hewitt, E.J. Mo as a Plant Nutrient: V. The interrelationships of molybdenum and nitrate supply in the concentration of sugars, nitrate and organic nitrogen in cauliflower plants grown in sand culture. *J. Hort. Sci.* **1955**, *30*, 151–162. [[CrossRef](#)]
33. Hewitt, E.J.; Bolle-Jones, E.W. Mo as a plant nutrient: I. The influence of Mo on the growth of some Brassica crops in sand culture. *J. Hort. Sci.* **1952**, *27*, 245–256. [[CrossRef](#)]
34. Eyster, C.; Brown, T.E.; Tanner, H.A.; Hood, S.L. Mn Requirement with Respect to Growth, Hill Reaction and Photosynthesis. *Plant Physiol.* **1958**, *33*, 235. [[CrossRef](#)]
35. Nable, R.O.; Loneragan, J.F. Translocation of Mn in subterranean clover (*Trifolium subterraneum* L. Cv. Seaton Park) I. redistribution during vegetative growth. *Funct. Plant Biol.* **1984**, *11*, 101–111. [[CrossRef](#)]
36. Kriedemann, P.E.; Graham, R.D.; Wiskich, J.T. Photosynthetic dysfunction and in vivo changes in chlorophyll a fluorescence from Mn-deficient wheat leaves. *Aust. J. Agric. Res.* **1985**, *36*, 157–169. [[CrossRef](#)]
37. Constantopoulos, G. Lipid metabolism of Mn-deficient algae: I. Effect of Mn deficiency on the greening and the lipid composition of *Euglena gracilis* Z. *Plant Physiol.* **1970**, *45*, 76–80. [[CrossRef](#)] [[PubMed](#)]
38. Wilson, D.O.; Boswell, F.C.; Ohki, K.; Parker, M.B.; Shuman, L.M.; Jellum, M.D. Changes in soybean seed oil and protein as influenced by Mn nutrition 1. *Crop Sci.* **1982**, *22*, 948–952. [[CrossRef](#)]
39. Henry, J.B.; Vann, M.; McCall, I.; Cockson, P.; Whipker, B.E. Nutrient disorders of burley and flue-cured tobacco. *Crop. Soils* **2018**, *51*, 44–52. [[CrossRef](#)]
40. Taylor, D.C.; Barton, D.L.; Rioux, K.P.; MacKenzie, S.L.; Reed, D.W.; Underhill, E.W.; Pomeroy, M.K.; Weber, N. Biosynthesis of acyl lipids containing very-long chain fatty acids in microspore-derived and zygotic embryos of *Brassica napus* L. cv Reston. *Plant Physiol.* **1992**, *99*, 1609–1618. [[CrossRef](#)]
41. Hoagland, D.R.; Arnon, D.I. The water-culture method for growing plants without soil. *Circ. Calif. Agric. Exp. Stn.* **1950**, 347.
42. Barnes, J.; Whipker, B.; McCall, I.; Frantz, J. Nutrient disorders of 'Evolution' mealy-cup sage. *HortTechnology* **2012**, *22*, 502–508. [[CrossRef](#)]
43. Bariya, H.; Bagtharia, S.; Patel, A.B. A promising nutrient for increasing growth and yield of plants. In *Nutrient Use Efficiency in Plants*; Hawkesford, M.J., Kopriva, S., De Kot, L.J., Eds.; Springer: Cham, Switzerland, 2014; pp. 153–170.
44. Henry, J.B. *Beneficial and Adverse Effects of Low Phosphorus Fertilization of Floriculture Species*; NCSU Library Repository: Raleigh, NC, USA, 2017.
45. Bryson, G.M.; Mills, H.A.; Sasseville, D.N.; Jones, J.B., Jr.; Barker, A.V. *Plant Analysis Handbook IV*; Micro-Macro Publ.: Athens, GA, USA, 2014.
46. Matoh, T.; Kobayashi, M. Boron and calcium, essential inorganic constituents of pectic polysaccharides in higher plant cell walls. *J. Plant Res.* **1998**, *111*, 179–190. [[CrossRef](#)]
47. Nuttall, W.F.; Ukrainetz, H.; Stewart, J.W.; Spurr, D.T. The effect of nitrogen, sulphur and B on yield and quality of rapeseed (*Brassica napus* L. and *B. campestris* L.). *Can. J. Soil Sci.* **1987**, *67*, 545–559. [[CrossRef](#)]
48. Popper, Z.A.; Fry, S.C. Xyloglucan–pectin linkages are formed intra-protoplasmically, contribute to wall-assembly, and remain stable in the cell wall. *Planta* **2008**, *227*, 781–794. [[CrossRef](#)]
49. Yang, M.; Shi, L.; Xu, F.S.; Wang, Y.H. Effect of B on dynamic change of seed yield and quality formation in developing seed of *Brassica napus*. *J. Plant Nutr.* **2009**, *32*, 785–797. [[CrossRef](#)]

50. Chen, G.; Clark, A.; Kremen, A.; Lawley, Y.; Price, A.; Stocking, L.; Weil, R. Brassicas and mustards. In *Managing Cover Crops Profitably*; USDA ARS: Washington, DC, USA, 2007; pp. 81–89.
51. Wu, J.; Schat, H.; Sun, R.; Koornneef, M.; Wang, X.; Aarts, M.G. Characterization of natural variation for Zn, Fe and Mn accumulation and Zn exposure response in *Brassica rapa* L. *Plant Soil* **2007**, *291*, 167–180. [[CrossRef](#)]
52. Ayala, M.B.; Sandmann, G. Activities of Cu-containing proteins in Cu-depleted pea leaves. *Physiol. Plant.* **1988**, *72*, 801–806. [[CrossRef](#)]
53. Khan, N.A.; Singh, S.; Nazar, R.; Lone, P.M. The source–sink relationship in mustard. *Asian Aust. J. Plant Sci. Biotechnol.* **2007**, *1*, 10–18.
54. Vallee, B.L.; Auld, D.S. Zn coordination, function, and structure of Zn enzymes and other proteins. *Biochemistry* **1990**, *29*, 5647–5659. [[CrossRef](#)]
55. Vallee, B.L.; Falchuk, K.H. The biochemical basis of Zn physiology. *Physiol. Rev.* **1993**, *73*, 79–118. [[CrossRef](#)] [[PubMed](#)]
56. Kochian, L.V. Mechanisms of Micronutrient Uptake and Translocation in Plants. *Methods Biogeochem. Wetl.* **2018**, *4*, 229–296.
57. Ajisaka, H.; Kuginuki, Y.; Yui, S.; Enomoto, S.; Hirai, M. Identification and mapping of a quantitative trait locus controlling extreme late bolting in Chinese cabbage (*Brassica rapa* L. ssp. *pekinensis* syn. *campestris* L.) using bulked segregant analysis. *Euphytica* **2001**, *118*, 75–81.
58. Cakmak, I.; Marschner, H. Increase in membrane permeability and exudation in roots of Zn deficient plants. *J. Plant Physiol.* **1988**, *132*, 356–361. [[CrossRef](#)]
59. Cakmak, I.; Marschner, H. Decrease in nitrate uptake and increase in proton release in Zn deficient cotton, sunflower and buckwheat plants. *Plant Soil* **1990**, *129*, 261–268. [[CrossRef](#)]
60. Vunkova-Radeva, R.; Schiemann, J.; Mendel, R.R.; Salcheva, G.; Georgieva, D. Stress and activity of Mo-containing complex (Mo cofactor) in winter wheat seeds. *Plant Physiol.* **1988**, *87*, 533–535. [[CrossRef](#)]
61. Jackson, C.; Dench, J.; Moore, A.L.; Halliwell, B.; Foyer, C.H.; Hall, D.O. Subcellular Localisation and Identification of Superoxide Dismutase in the Leaves of Higher Plants. *JBC J. Biol. Inorg. Chem.* **1978**, *91*, 339–344. [[CrossRef](#)]
62. Osborne, G.J.; Pratley, J.E.; Stewart, W.P. The tolerance of subterranean clover (*Trifolium subterraneum* L.) to aluminium and manganese. *Field Crops Res.* **1980**, *3*, 347–358. [[CrossRef](#)]
63. Brown, P.H.; Graham, R.D.; Nicholas, D.J. The effects of Mn and nitrate supply on the levels of phenolics and lignin in young wheat plants. *Plant Soil* **1984**, *81*, 437–440. [[CrossRef](#)]